International Journal of GEOMATE, March, 2020, Vol.18, Issue 67, pp. 90-95
ISSN: 2186-2982 (P), 2186-2990 (O), Japan, DOI: https://doi.org/10.21660/2020.67.5789
Special Issue on Science, Engineering and Environment

LOCALIZED PLASTIC DEFORMATION AND PERIODIC TABLE

Lev Zuev[1], *Svetlana Barannikova[1] and Albina Nikonova[1]

[1]Strength Physics Laboratory, Institute of Strength Physics & Materials Science SB RAS, Russia

*Corresponding Author, Received: 13 June 2019, Revised: 15 Oct. 2019, Accepted: 09 Jan. 2020

ABSTRACT: We consider the autowave mechanism of evolution of a localized plastic deformation of crystalline solids of different origins. It is found that localization of the plastic flow is determined by the relation between elastic and plastic phenomena in deforming materials. The origin of this relation is explained using general thermodynamic concepts. It is shown that parameters of plastic flow localization at the stage of linear strain hardening in the process of solid body deformation are closely related to characteristics of the electronic structure of metals. Inverse of the product of wavelength and velocity of the localized plasticity autowave grows linearly with the number of conduction electrons per unit cell of the metal. The obtained data directly indicate that the nature of the electron-gas contribution to hindering of dislocations is more complicated. Thus, the parameters of plastic flow localization are defined by the position of metal in the Mendeleev periodic table.

Keywords: Plastic deformation, Autowave, Pattern, Electronic structure, Periodic Table

1. INTRODUCTION

Plastic deformation of solids is a complex physical phenomenon the evolution of which depends on the crystal lattice and crystal structure defects. The process of plastic flow is usually described by the dependence σ(ε) of the deforming stress on the strain. It is important that at all its stages from the beginning of plastic flow (yield stress) to fracture (ultimate strength), this process is accompanied by plastic strain localization [1].

The model of evolution of localized plastic strain proposed in [1] presumes that self-organization of the defect structure [2] occurs in the form of autowaves of a localized plastic flow [1,3], which appear in the deforming medium as a result of interaction of elastic waves and relaxation events of breaking of elastic stress concentrators. Each relaxation event contributes to the overall plastic deformation and generates new stress concentrators. The autowave pattern of localized plasticity distribution regularly changes in accordance with the stage nature of the σ(ε) curve so that the deformation process can be treated as a natural evolution of localized plasticity autowaves [1].

Therefore, autowaves (localized plasticity) and wave (elastic) deformation phenomena coexist in a plastically deforming medium. The former are characterized by wavelength λ of the localized plasticity autowave and velocity V_{aw} of its propagation, while the latter are determined by the interplanar distance χ in the crystal lattice of the tested material and the velocity V_t of propagation of transverse elastic waves.

It was noted in earlier experiments with a number of metals [1,4,5] that dimensionless ratio $\lambda V_{\mathrm{aw}}/\chi V_{\mathrm{t}}$ formed by these four characteristics is the same for all cases of straining of different metals at the stages of linear strain-hardening when σ ~ ε. This suggested that ratio $\lambda V_{\mathrm{aw}}/\chi V_{\mathrm{t}}$ is invariant in general. This study aims at the verification of this regularity not only for metals, but also for other materials with a linear law hardening. It is also important to clarify the origin of this relation using general thermodynamic concepts.

2. EXPERIMENTAL DATA

Experimental investigations of localized plastic flow were carried out for different metals related to periods 3–6 of Mendeleev's Periodic Table (see Table 1). The quantitative data on the localized plasticity patterns were estimated experimentally for linear stages of the processes at which the deforming stresses and strains are connected by a linear relation. In these cases, a phase localized plasticity autowave corresponding to the condition of the constancy of phase $2\pi(t/T - x/\lambda) = const$ is observed, where T is the period of oscillations in the wave, x is the coordinate, and t is the running time. The localized plasticity pattern formed in such cases is stable and can be observed relatively easily [1].

For estimating ratio $\lambda V_{\mathrm{aw}}/\chi V_{\mathrm{t}}$ characterizing various materials, the range of metals under investigation was extended. In addition, we studied the localization of plastic deformation in alkali-halide crystals (KCl, NaCl, and LiF) and rocks such as sandstone (SiO_2) and marble ($CaCO_2$). To observe localization patterns, the method combining mechanical tests with double-exposure speckle photography (DESP) adapted for plastic deformation was used. This allowed the displacements vector field r (*x*,*y*) arising on the flat sample surface to be reconstructed for step-by-step strain increase by δε ≈

10^{-3}at any stage of the process and the components of plastic distortion tensor to be calculated. The DESP method for observing the patterns of a localized plastic flow in deforming materials, which was based on speckle photography, was described in detail earlier [1] and will not be discussed here. For illustrating the potentialities of this method, Fig. 1 shows a typical pattern of local plasticity distribution for sequential stages of easy slip and linear strain-hardening during tension with a constant rate for a single crystal sample of alloy Fe-12 wt %Mn (γ-Fe).

Table 1 Metals under study

Period		Metals						
3	Element	Mg	Al					
	Atomic number	12	13					
4	Element	Ti	V	Fe	Co	Ni	Cu	Zn
	Atomic number	22	23	26	27	28	29	30
5	Element	Zr	Nb	Mo	Cd	In	Sn	
	Atomic number	40	41	42	48	49	50	
6	Element	Hf	Ta	Pb				
	Atomic number	72	73	82				

3. RESULTS AND DISCUSSION

The quantitative characteristics λ and V_{aw} required for analyzing the data on the evolution of localized plasticity were determined from the processing of the so-called *X–t* diagrams proposed in [1] for such purposes and shown in Fig. 2. It can be seen from the figure that the values of autowave wavelength λ and period T can be determined from the vertical and horizontal sections of families of the $X(t)$ curves. Characteristics λ and $V_{aw} = \lambda/T$ of localized plasticity autowaves were determined for linear work-hardening of metals, easily slip in metal single crystals, compression of rock samples, and the phase-transformation straining of the NiTi single crystal.

Let us analyze the data obtained in these experiments. The values of products λV_{aw} for 19 tested metals are given in Table 2. It can be seen that the results differ insignificantly and the mean value of the product of these quantities is $\langle \lambda V_{aw} \rangle_{lwh} = (2.52 \pm 0.36) \times 10^{-7}$ m^2/s.

We managed to supplement these data with the results of analogous processing of localized plasticity patterns observed at the easy slip stages in Cu, Ni, a-Fe, γ-Fe, Zn, and Sn single crystals for which the proportionality σ ~ ε also holds and a phase autowave is observed. For this stage, we have $\langle \lambda V_{aw} \rangle_{eg} \sim (2.95 \pm 1.05) \times 10^{-7}$ m^2/s (see Table 2).

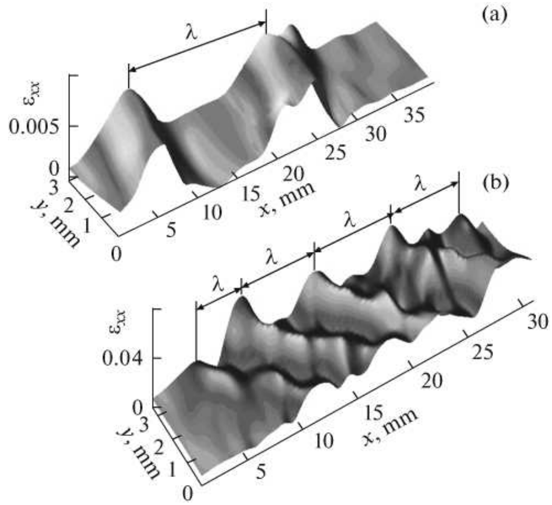

Fig. 1 Strain distribution over a sample of Fe-12 wt %Mn alloy (a) at the easy slip state and (b) at the linear work hardening stage.

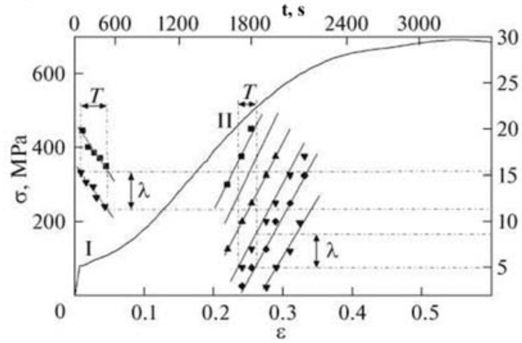

Fig. 2 *X–t* diagram for Hadfield steel single crystal, plotted for the case shown in Fig. 1.

The stage of linear work-hardening and corresponding localized plasticity phase autowaves were observed for compressed samples of alkali-halide crystals and rocks [6,7]. The results of these experiments given in Table 3 lead to $\langle \lambda V_{aw} \rangle_{abc} = (3.44 \pm 0.49) \times 10^{-7}$ m^2/s and $\langle \lambda V_{aw} \rangle_{rock} = (1.44 \pm 0.34) \times 10^{-7}$ m^2/s.

In the case of staining due to the slip of individual dislocations, the process is usually characterized by dislocation path length l and dislocation velocity V_{disl}; these parameters were determined from analysis of the available data on the mobility of individual dislocations in single crystals [8-12] in the quasi-viscous flow regime, in which $V_{disl} \sim \sigma$ [13]. In such conditions, the characteristic dislocation path lengths lie in the interval 10^{-5} m ≤ l ≤ 10^{-4} m and the velocities of dislocations belong to the range 10^{-3} m/s ≤ V_{disl} ≤ 10^{-2} m/s. The product of these quantities was estimated using the relation $lV_{disl} = V_{disl}^2\tau$, where τ is the duration of the load pulse acting during the crystal loading. The results of calculations of products lV_{disl} in these cases are given in Table 4. It can be seen that $\langle lV\rangle_{disl} = (3.2 \pm 0.35) \times 10^{-7}$ m²/s in this case.

Table 2 Comparison of quantities χV_t and λV_{aw} for metals

×10⁷ m²/s	Linear strain hardening stage												
	Cu	Zn	Al	Zr	Ti	V	Nb	α-Fe	γ-Fe	Ni	Co	Mo	
λV_{aw}	3.6	3.7	7.9	3.7	2.5	2.8	1.8	2.55	2.2	2.1	3.0	1.2	
χV_t	4.8	11.9	7.5	11.9	7.9	6.2	5.3	4.7	6.5	6.0	6.0	7.4	
$\lambda V_{aw}/\chi V_t$	0.75	0.3	1.1	0.3	0.3	0.45	0.33	0.54	0.34	0.35	0.5	0.2	
×10⁷ m²/s	Linear strain hardening stage							Easy slip stage					
	Sn	Mg	Cd	In	Pb	Ta	Hf	α-Fe	γ-Fe	Cu	Zn	Ni	Sn
λV_{aw}	2.4	9.9	0.9	2.6	3.2	1.1	1.0	7.4	2.9	1.9	1.0	1.3	3.3
χV_t	5.3	15.8	3.5	2.2	2.0	4.7	4.2	6.5	6.0	4.7	5.0	6	4.9
$\lambda V_{aw}/\chi V_t$	0.65	0.63	0.2	1.2	1.6	0.2	0.24	1.1	0.49	0.4	0.2	0.2	0.67

The experimental estimation of the parameters of a localized plasticity autowave for plastic deformation of TiNi intermetallide single crystal of the equiatomic composition (strain-induced phase transformation [14]) resulted in the value $\langle\lambda V_{aw}\rangle_{pt} \approx 0.85 \times 10^{-7}$ m²/s.

Table 3 Comparison of quantities χV_t and λV_{aw} for alkali- halide crystals [6] and rocks [7]

x10⁷ m²/s	KCl	NaCl	LiF	Marble	Sandstone
λV_{aw}	3.0	3.1	4.3	1.75	0.6
χV_t	7.0	7.5	8.8	3.7	1.5
$V_{aw}/\chi V_t$	0.43	0.4	0.5	0.5	0.4

Comparing pairwise the above data by calculating the Student t-test [15], we can conclude that the resultant values differ insignificantly (i.e., belong to the same general population). This leads to

$$\langle\lambda V_{aw}\rangle_{lwh} \approx \langle lV\rangle_{disl} \approx \langle V_{aw}\rangle_{pt} \approx \langle V_{aw}\rangle_{abc} \approx \langle V_{aw}\rangle_{rock} \quad (1)$$

Table 4 Comparison of quantities χV_t and lV_{disl} determined by measuring of path lengths of individual dislocations

×10⁷ m²/s	NaCl [8]	LiF [9]	CsI [10]	KCl [11]	Zn [12]
lV_{disl}	4.1	4.1	1.9	4.1	1.8
χV_t	7.3	8.6	4.0	6.8	4.0
$lV_{disl}/\chi V_t$	0.56	0.47	0.47	0.6	0.45

Elastic processes in the tested materials were characterized by interplanar distances χ in the crystal lattice [16] and velocities V_t of propagation of transverse elastic waves [17]. As follows from Tables 2-4, we have $\langle\chi V_t\rangle_{el} = (5.8 \pm 0.3) \times 10^{-7}$ m²/s for all tested materials.

Analysis of the data array obtained for stages of linear strain hardening made it possible to establish that the dependence of λV_{aw} on atomic number of the element Z oscillates with respect to the average value with increasing number of the element within the limits of $13 \le Z \le 82$.

It has been found that these oscillations correlate with regularities in the behavior with an increase in Z of some independently determined lattice characteristics such as, e.g., characteristic Debye temperature $\Theta_D \approx \hbar\omega_D/k_B$ ($\hbar = h/2\pi$ is the Planck constant, ω_D is the Debye frequency, and k_B is the Boltzmann constant) [16], density, melting temperature, elastic moduli, and ionization potential [17].

As an example, correlation of the discussed dependences is illustrated by the common mode behavior of the quantities λV_{aw} binding energy E_b and Θ_D as functions of the atomic number of the elements under study (Fig. 3).

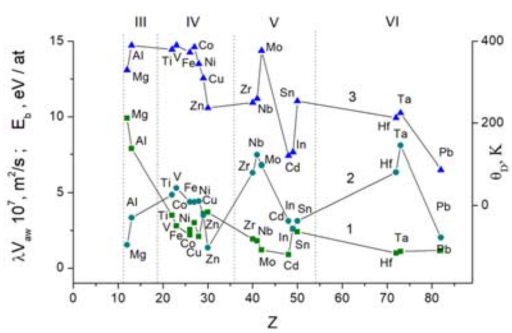

Fig. 3 The quantity (1) λV_{aw}, binding energy E_b (2) and (3) Debye temperature Θ_D as functions of atomic number of elements Z (III, IV, V, and VI are numbers of periods)

In addition, in analyzing the behavior of the product λV_{aw} within the limits of each period of Mendeleev's periodic law, it has been found that the quantity $(\lambda V_{aw})^{-1}$ grows linearly with the number of conduction electrons per unit cell of the metal n [18]; therefore, the relation

$$(\lambda V_{aw})^{-1} = A + \mathrm{B} \cdot \mathrm{n} \tag{2}$$

where A and B are constants different for periods 3, 4, 5, and 6, is valid in each period. The dependences established for the abovementioned periods are shown in Fig. 4.

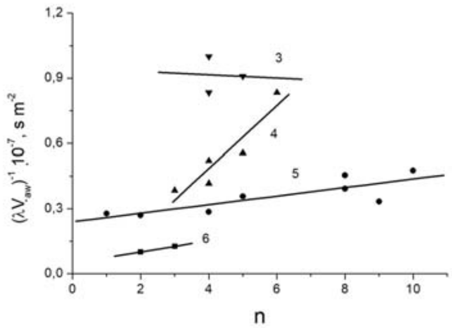

Fig. 4 The quantity $(\lambda V_{aw})^{-1}$ as a functions of number of conduction electrons per unit cell n (3, 4, 5, and 6 are numbers of periods)

It was also noted that the parameter of plasticity λV_{aw} correlates with different physical properties, as shown in Fig.5 a-b. The correlation coefficient: (a) R=1; 0,6; 0,6; 0,9; (b) R=1; 0,53; 0,4; 0,95.

In this case, the dependencies are presented in the form of four linear dependencies, which covers a metals related to the 3rd, 4th, 5th and 6th periods of Mendeleev periodic table respectively.

The existence of a linear relation such as (Eq.2) was already noted in [19]; however, the separation by periods of Mendeleev's Table was not observed earlier. Processing of experimental data for elements of periods 4–6 shows that,

$$B = A \cdot \exp(\beta / N), \tag{3}$$

where A and B are constants. In relation (3), N = 4, 5, and 6 is the period number in Mendeleev's periodic law (it is well known [20] that the number of the period coincides with the number of electron shells of its atoms) and в is a constant.

It has been found that the quantity λV_{aw} grows linearly with normalized the Debye temperature Θ_D [17, 18]; therefore, the relation

$$\lambda V_{aw} = A \cdot \Theta_D \cdot \frac{k_B}{\mathrm{Eb}}, \tag{4}$$

where constant $A = 4.42 \times 10^{-5}$ m^2/s, E_b is binding energy and k_B is the Boltzmann constant.

The dependence established for the abovementioned periods is shown in Fig. 6.

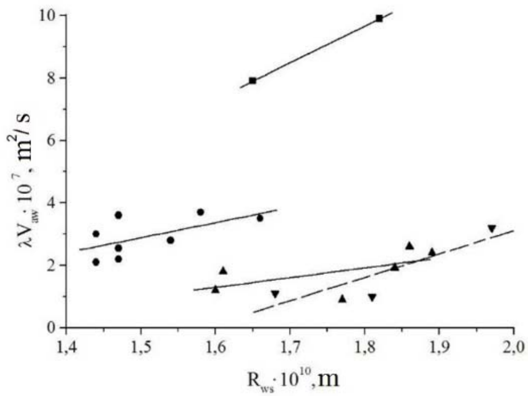

a)

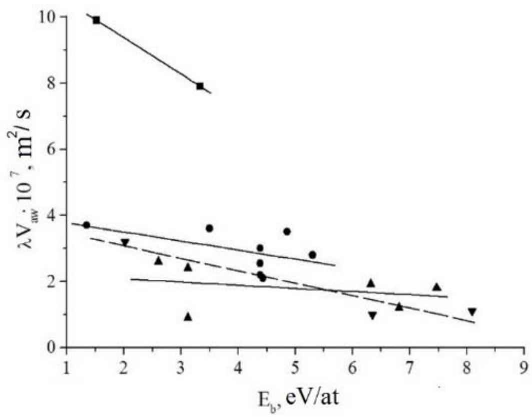

b)

Fig. 5 The dependence of parameter of plasticity on Wigner–Seitz radius (a), the bond energy (b), ■ – elements of the 3rd period (Mg, Al), ● – elements of the 4th period (Ti, V, α-Fe, γ-Fe, Co, Ni, Cu, Zn), ▲ – elements of the 5th period периода (Zr, Nb, Mo, Cd, In, Sn); ▼ – elements of the 6th period (Hf, Ta, Pb).

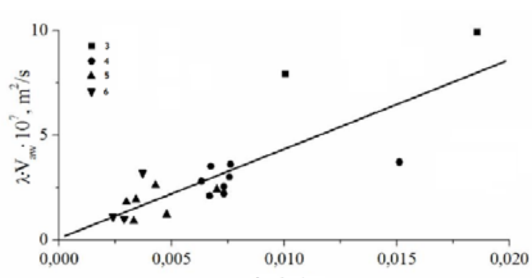

Fig. 6 The quantity λV_{aw} as a function of normalized the Debye temperature Θ_D (3, 4, 5, and 6 are numbers of periods)

The coefficient of correlation between the quantities presented in Fig. 4 is ~0.96, which indicates the existence of a functional relationship between them [15].

4. CONCLUSIONS

The obtained data testify that parameters of plastic flow localization at the stage of linear work hardening in the process of solid body deformation are closely related to characteristics of the electronic structure of metals. This relation manifests itself as a dependence of macroscopic characteristics of localized plasticity autowave propagation at the stage of linear strain hardening on the period number in Mendeleev's Table. In addition, these characteristics depend on the number of valence electrons; for most metals but transition ones, it coincides with the group number in the periodic system. The obtained data directly indicate that the nature of the electron-gas contribution to hindering of dislocations is more complicated than is envisaged in existing theories [21] of this effect.

The elastic-plastic invariant necessitates the allowance for the role played by elastic (lattice) characteristics of materials and is important in the development of models [22-32] and mechanisms of evolution of a plastic flow [33-42].

5. ACKNOWLEDGMENTS

This work was performed by the financial support of RSF, grant no. 16-19-10025 P.

6. REFERENCES

[1] Zuev L. B., Danilov V. I., Barannikova S. A., and Zykov I. Y., A new type of plastic deformation waves in solids, Applied physics A-Materials Science & Processing, Vol.71, Issue 1, 2000, pp. 91-94.

[2] Seeger A. and Frank W., Structure Formation by Dissipative Processes in Crystals with High Defect Densities, Non-Linear Phenomena in Material Science, Ed. by L. P. Kubin and G. Martin, New York, Trans Tech, 1987, pp. 125-138.

[3] Davydov V. A., Davydov N. V., Morozov V. G., Stolyarov M. N., and Yamaguchi T., Autowaves in moving excitable media, Condensed Matter Physics, Vol. 7, Issue 3, 2004, pp.565-578.

[4] Barannikova S. A., Nadezhkin M. V., Mel'nichuk V. A., and Zuev L. B., Tensile plastic strain localization in single crystals of austenite steel electrolytically saturated with hydrogen, Technical Physics Letters, Vol. 37, Issue 9, 2011, pp. 793-796.

[5] Barannikova S., Zuev L., and Li Y., Plastic flow heterogeneity and failure of bimetal material, International Journal of GEOMATE, Vol. 14, Issue, 43, 2018, pp. 112-117.

[6] Barannikova S. A., Nadezhkin M. V., and Zuev L. B., Relationship between burgers vectors of dislocations and plastic strain localization patterns in compression-strained alkali halide crystals, Technical Physics Letters, Vol. 37, 2011, p. 750.

[7] Zuev L. B., Barannikova S. A., Nadezhkin M. V., and Gorbatenko V. V., On the Observation of Slow Wave Processes in Deforming Rock Sample, Journal of Mining World Express, Vol.2, Issue 1, 2013, pp. 31-39.

[8] Kurilov V. F., Zuev L. B., Gromov V. E., Sergeev V. P., and Gershtein G. I., Dynamic Deceleration of Dislocations in NaCl Crystals of Different Purity, Kristallografiya 22, 1977, pp. 653-654.

[9] Darinskaya E. V., Urusovskaya A. A., Opekunov V. N., Abramchuk G. A., and Alekhin V. F., Study of Viscous Deceleration of Dislocations in LiF Crystals Based on the Mobility of Individual Dislocations, Fizika Tverdogo Tela, Vol. 20, 1978, p. 1250-1252.

[10] Darinskaya E. V. and Urusovskaya A. A., Viscous Deceleration of Dislocations in CsI Crystals at a Temperature of 77–300 K, Fizika Tverdogo Tela, Vol. 17, 1975, pp. 2421-2422.

[11] Zuev L. B., Gromov V. E., and Aleksankina O. I., Dependence of Dislocation Velocity on Electric Field Intensity, Kristallografiya, Vol. 19, 1974, pp. 889-891.

[12] Zuev L. B., Gromov V. E., Kurilov V. F, and Gurevich L. I., Mobility of Dislocations in Zn Single Crystals Under the Action of Current Pulses, Dokl. Akad. Nauk SSSR, Vol. 239, 1978, pp. 874-876.

[13] Al'shits V. I. and Indenbom V. L., Dislocations in Solids, Ed. by F. R. N. Nabarro, Amsterdam Elsevier, 1986, p. 1-43.

[14] Otsuka K. and Shimizu K., Pseudoelasticity and shape memory effects in alloys, International Metals Reviews, Vol. 31, Issue 3, 1986, pp. 93.

[15] Hudson D. J., Lectures on Elementary Statistics and Probability, Geneva CERN, 1963, pp.1-105.

[16] Newnham R. E., Properties of Materials, Oxford Univ. Press, 2005, pp. 1-391.

[17] Grigorovich V. K., Metallography and Heat Treatment, The Handbook, Ed. by M. L. Bernshtein and A. G. Rakhshtadt, Moscow, Metallurgizdat, 1961, in Russian, p. 387.

[18] Cracknell A. P. and Wong K. C., The Fermi Surface, Oxford, Clarendon Press, 1973, pp. 1-565.

[19] Zuev L. B., The linear work hardening stage and de Broglie equation for autowaves of localized plasticity, International Journal of Solids and Structures, Vol. 42, 2005, pp. 943-949.

[20] Shpol'skii E. V., Atomic Physics, Vol. 1, Moscow, Nauka, 1974, in Russian, pp. 1-571.

[21] Suzuki T., Takeuchi S., and Yoshinaga H., Dislocation Dynamics and Plasticity, Berlin, Springer, 1991, pp. 1-227.

[22] Naimark O. B., Defect induced transitions as mechanisms of plasticity and failure in multifield continua, Advances in Multifield Theories of Continua with Substructure, Boston, Birkhauser Inc., 2003, pp. 75–114.

[23] Zbib H. M., de la Rubia T. D., A multiscale model of plasticity, International Journal of Plasticity, Vol. 18, Issue 7, 2002, pp. 1133–1163.

[24] Ohashi T., Kawamukai M., and Zbib H., A multiscale approach for modeling scale-dependent yield stress in polycrystalline metals, International Journal of Plasticity, Vol. 23, Issue 5, 2007, pp. 897–914.

[25] Zaiser M., and Aifantis E. C., Randomness and slip avalanches in gradient plasticity, International Journal of Plasticity, Vol. 22, Issue 8, 2006, pp. 1432–1455.

[26] Bilalov D. A., Sokovikov M. A., Chudinov V. V., Oborin V. A., Bayandin Y. V., Terekhina A. I., and Naimark O. B., Numerical Simulation and Experimental Study of Plastic Strain Localization under the Dynamic Loading of Specimens in Conditions Close to a Pure Shear, Journal of Applied Mechanics and Technical Physics, Vol. 59, Issue 7, 2018, pp. 1179-1188.

[27] Naimark O. B., Bayandin Y. V., and Zocher M. A., Collective properties of defects, multiscale plasticity, and shock induced phenomena in solids, Physical Mesomechanics, Vol. 20, Issue 1, 2017, pp. 10-30.

[28] Zhelnin M., Iziumova A., Vshivkov A., and Plekhov O., Experimental study of an effect of plastic deformation on thermal properties of stainless steel, Quantitative InfraRed Thermography Journal, Vol. 16, Issue 1, 2019, pp. 74-86.

[29] Moretti P., Renner J., Safari A., and Zaiser M., Graph theoretical approaches for the characterization of damage in hierarchical materials, European Physical Journal B, Vol. 92, Issue 5, 2019, pp.97:1.

[30] Wu R., Tüzes D., Ispánovity P. D., Groma I., Hochrainer T., and Zaiser M., Instability of dislocation fluxes in a single slip: Deterministic and stochastic models of dislocation patterning, Physical Review B, Vol.98. Issue 5, 2018, pp. 054110:1.

[31] Valdenaire P. L., Le Bouar Y., Appolaire B., and Finel A., Density-based crystal plasticity: From the discrete to the continuum, Physical Review B, Vol. 93, Issue 21, 2016, pp. 214111:1.

[32] Xia S., and El-Azab A., Computational modelling of mesoscale dislocation patterning and plastic deformation of single crystals, Modelling and Simulation in Materials Science and Engineering, Vol. 23, Issue 5, 2015, pp. 055009:1.

[33] Lebyodkin M. A., Kobelev N. P., Bougherira Y., Entemeyer D., Fressengeas C., Gornakov V. S., Lebedkina T. A., and Shashkov I. V., On the similarity of plastic flow processes during smooth and jerky flow: Statistical analysis, Acta Materialia, Vol. 60, Issue 9, 2012, pp. 3729-3740.

[34] Fressengeas C., and Taupin V., A field theory of strain/curvature incompatibility for coupled fracture and plasticity, International Journal of Solids and Structures, Vol. 82, 2016, pp. 16-38.

[35] Lebyodkin M. A., Zhemchuzhnikova D. A., Lebedkina T. A., and Aifantis E. C., Kinematics of formation and cessation of type B deformation bands during the Portevin-Le Chatelier effect in an AlMg alloy, Results in Physics, Vol. 12, 2019, pp. 867-869.

[36] Zuev L. B., Barannikova S. A., Lunev A. G., Kolosov S. V., and Zharmukhambetova A. M., Basic Relationships of the Autowave Model of a Plastic Flow, Russian Physics Journal, Vol. 61, Issue 9, 2019, pp. 1709-1717.

[37] Zuev L. B., Lunev A. G., Barannikova S. A., and Staskevich O. S., Plastic Flow Localization and Strain Hardening of Metals, Russian Metallurgy, Vol. 2019, Issue 4, 2019, pp. 273–280.

[38] Zuev L. B., Barannikova S. A., and Maslova O. A., The features of localized plasticity autowaves in solids, Materials Research, Vol. 22, Issue 4, 2019, pp. e20180694:1-12.

[39] Zuev L. B., Barannikova S. A., and Li Yu. V., The kinetics of deformation localization nuclei for the coarse-grained Fe-3%Si alloy, Materials Today: Proceedings, Vol. 5, Issue 1P1, 2018, pp. 1121-1124.

[40] Lunev A. G., Nadezhkin M. V., Barannikova S. A., and Zuev L. B., Acoustic Parameters as Criteria of Localized Deformation in Aluminum Alloys, Acta Physica Polonica A, Vol. 134, Issue 1, 2018, pp. P. 342-345.

[41] Barannikova S., Li Yu., and Zuev L., Research of the plastic deformation localization of bimetal, Metalurgija, Vol. 57, Is. 4, 2018, pp. 275-278.

[42] Li Yu. V., Zharmukhambetova A. M., Barannikova S. A., and Zuev L. B., On the macroscopic phenomena of plastic flow localization and solids microscopic characteristics, Journal of Physics: Conference Series. Vol. 1115, 2018, pp. 042037:1-5

[43]